Nondestructive evaluation of Microstructure and Stresses in Steels

T. Jayakumar and Anish Kumar
Metallurgy and Materials Group
Indira Gandhi Centre for Atomic Research, Kalpakkam, Tamil Nadu-603102, India

ABSTRACT

The paper presents an overview of the nondestructive methodologies developed at the authors' laboratory for characterization of microstructural features in various steels such as ferritic, austenitic stainless and maraging steels. The emphasis is given on the judicious selection of a single non destructive evaluation non destructive evaluation (NDE) technique/parameter or multi-technique/ multi-parameteric approach for comprehensive characterization of microstructural/ substructural changes occurring in steels, based on the in-depth understanding of the materials response to the specific form of energy imparted during NDE.

INTRODUCTION

Material researchers over the years have developed a range of physical, chemical, mechanical and microstructural characterization techniques to cater to varying needs of a wide variety of materials and performance evaluation. Material characterization by nondestructive evaluation (NDE) techniques finds favour for the assessment of microstructures and mechanical properties after initial heat treatment as a quality control measurement and their subsequent degradation during service such as exposure to high temperature in addition to static and/ or cyclic loading [1]. Interaction of probing media/ energy with the material provides information about the material, in terms of the influence of material properties on propagation of the probing media in the material. In the case of ultrasonic characterization of materials, velocity and attenuation of ultrasonic wave through the material is governed by the elastic properties of the material, and scattering and absorption in the material respectively. In the case of eddy current evaluation, the generation and propagation of eddy currents in the material are function of conductivity and permeability of the material. Magnetic parameters, such as hysteresis loop parameters and magnetic Barkhausen emission (MBE), have also emerged as viable NDE technique for microstructural characterization in ferromagnetic materials. The magnetic parameters are influenced by various microstructural features such as volume fraction of ferromagnetic/ paramagnetic phases, precipitation and dislocation density. These typically show the basis for materials characterization using NDE parameters.

The interaction of a nondestructive probing medium with a material depends on various substructural and microstructural features such as point defects, dislocations, voids, micro and macro cracks, secondary phases, texture, residual stress etc. While this is considered as advantageous for complete characterization, many a time such comprehensive interaction of the probing medium with various microstructural features may lead to complex signals, thus making interpretations very difficult and requiring unfolding the signal to obtain the feature specific information. Further, each technique has its own strengths and weaknesses depending upon the interaction of the probing medium with the material microstructure/ substructure. Under such conditions, use of multiple NDE techniques and multiple NDE parameters in a complementary manner helps in isolating the influence of one or a combination of specific microstructural features. Understanding the interaction of NDE probing medium and the material greatly helps in evolving new concepts and the specialized approaches in the analysis of NDE signal towards application in characterization of materials.

The present paper demonstrates the comprehensive characterization of microstructural/ substructural changes occurring in steels by judicious selection of a single NDE technique/parameter or multi-technique/ multi-parameteric approach, based on the in-depth understanding of the materials response to the specific form of energy imparted during NDE. It is shown that the ultrasonic velocity is sensitive to the volume fraction of various phases, whereas the attenuation of ultrasonic wave is more sensitive to the grain size variations in ferritic steel. In M250 maraging steel, it is shown that the ultrasonic velocity is a better parameter for characterization of precipitation behavior, whereas, magnetic Barkhausen emission technique is more sensitive to the reversion of austenite. Further, positron annihilation technique can be used for studying the annihilation and generation of defects during the initial and intermediate stages of ageing of the maraging steel respectively. MBE has been used for characterization of tensile deformation, fatigue damage and stress in ferritic steels, whereas ultrasonic velocity is found to be very effective for characterization of texture and recrystallization behavior in austenitic stainless steel due to its high elastic anisotropy. The high elastic anisotropy of austenitic stainless steel also makes it a highly scattering material, and hence ultrasonic attenuation measurements can be used more effectively for grain size measurement in austenitic stainless steels as compared to ferritic steels. Further, thermomechanical processing that leads to change in the grain size and its distribution can also be characterized effectively using ultrasonic attenuation measurements in austenitic stainless steel. Eddy current technique has been used for detecting the presence of delta-ferrite (a magnetic phase) in austenitic stainless steel weldment and characterization of sensitization in austenitic stainless steel. Various case studies describing the above are presented in the following sections.

Microstructural Characterization in Modified 9Cr-l Ferrite Steel Using Ultrasonics

Modified 9Cr-1Mo steel (T91/ P91), with high creep strength and thermal conductivity, low thermal expansion coefficient and good resistance to corrosion and stress corrosion cracking, is widely used as a structural material in power generating and petrochemical industries. The alloy is recommended for use in the normalized and tempered condition. Because of transformable nature

of the ferritic alloy, it is susceptible to the formation of undesirable microstructures during fabrication and/or heat treatment processes. It is important to nondestructively characterize the microstructure of this steel for quality control during fabrication and heat treatment to ensure the desired microstructure and mechanical properties. Ultrasonic technique offers promise in this regard.

Characterization of solution annealing behaviour

Ultrasonic velocity and attenuation measurements and spectral analysis of the first back wall echo have been used for characterization of microstructures obtained by various heat treatments in modified 9Cr-1Mo ferritic steel (T91/P91) [2]. The heat treatments consist of soaking the material for 5 minutes at selected temperatures starting from ? phase region (1073 K) to ? + ? phase region (1623 K), followed by oil quenching. Ultrasonic longitudinal and shear wave velocities decreased with increase in soaking temperature in the intercritical region, due to the increased amount of martensite (Fig. 1a). Ultrasonic velocities are found to be useful in identifying the Ac1 and Ac3 temperatures and also for the determination of hardness in the intercritical region. Ultrasonic attenuation measurements are found to be useful to characterize the variation in the prior austenitic grain size and formation of ?-ferrite above Ac4 temperature. Two distinct peaks at around 7.0 MHz and 17.0 MHz have been observed in the autopower spectra of the first back wall echoes of all the specimens heat treated at different soaking temperature, when 20 MHz longitudinal beam transducer was used [3]. The variation in the ratio of these two peaks (amplitude of lower frequency peak / amplitude of higher frequency peak) with soaking temperature exhibited almost similar behaviour as that of ultrasonic attenuation. A linear correlation between the SPR and the grain size is found to be valid for a wide range of microstructures, i.e. ferrite, ferrite + martensite and martensite (Fig. 1b). The use of SPR for grain size measurements has a distinct advantage over the other ultrasonic methods because (1) the SPR is not influenced by the couplant condition and (2) this methodology needs only the first back wall echo, hence it can be used on highly attenuating and thick materials also.

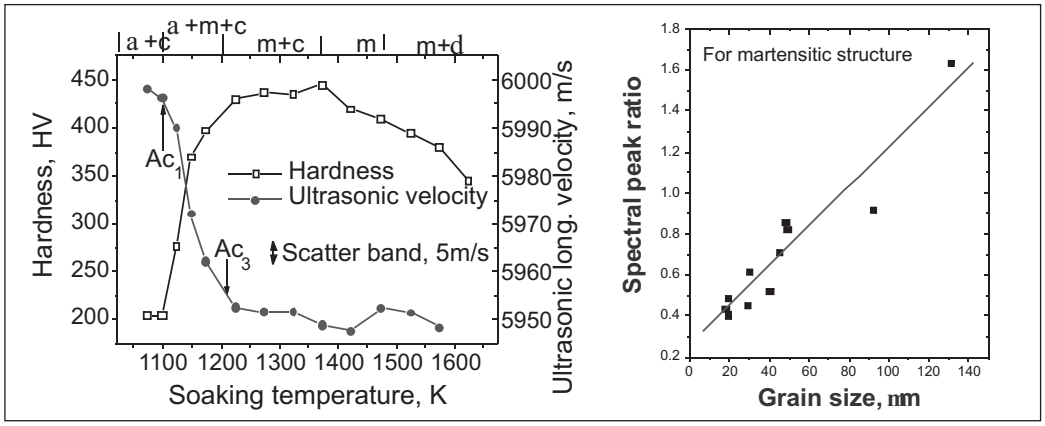

(a) (b)

Fig. 1: Variations in (a) hardness and ultrasonic longitudinal wave velocity with soaking temperatures and (b) spectral peak ratio with grain size, in modified 9Cr-1Mo ferritic steel.

Imaging of weldments and assessment of PWHT

At elevated temperatures, the performance of Cr-Mo steel weldments is considered to be a life limiting factor and a high percentage of failures have been reported to be weld related. As the microstructure in the as-welded condition is predominantly martensitic in both heat affected zone (HAZ) and weld metal, proper post weld heat treatment (PWHT) is required to be carried out to temper the microstructure and thus improve the toughness of the weld. To ensure suitable microstructure and mechanical properties after PWHT, a non-destructive technique based evaluation is required. Ultrasonic velocity measurements have been carried out to get the weld profile and to assess the adequacy of PWHT in modified 9Cr-1Mo ferritic steel weldments. Ultrasonic velocity measurements across the weld in the as-welded condition revealed that ultrasonic velocity is maximum in the parent metal and minimum in the weld metal (Fig. 2). As the amount of weld metal increased in the propagation direction of ultrasonic beam, ultrasonic velocity decreased and hence the amount of weld metal and parent metal could be determined in the propagation direction of ultrasonic beam, which could be used in-turn to get the weld profile. The ultrasonic velocity plot was found to almost replicate the weld profile. The lower velocity in the weld metal is due to the presence of martensitic structure with lower ultrasonic velocity. After PWHT (1033 K for 1h), ultrasonic velocity in the weld metal is found to be slightly lower than that in parent metal but is higher than that in the weld metal in the as welded condition. Hence the adequacy of PWHT can be assessed using ultrasonic velocity and the weld profile can also be determined even after the PWHT condition.

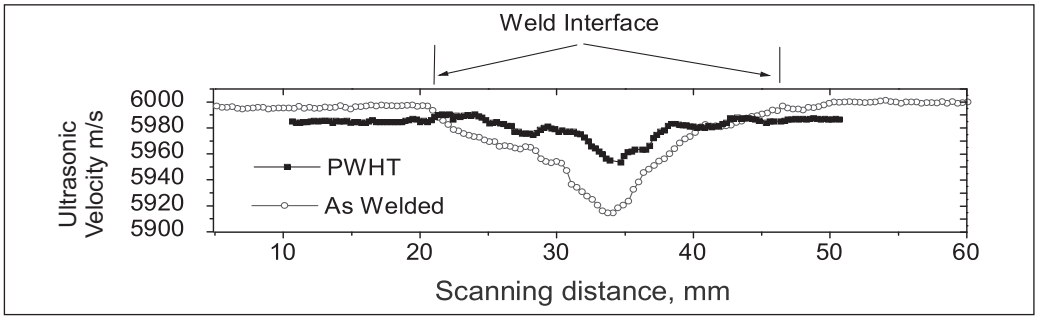

Fig. 2: Variation in ultrasonic longitudinal wave velocity with scanning distance across the weld-line in as-welded and PWHT weldments

Early detection of Type-IV cracking in creep tested weldments

Operational experience obtained from the usage of modified 9Cr-1Mo ferritic steel weldment at high temperature shows that failures in steel weldments are due to type IV cracking in heat affected zone (HAZ) near the base metal in intercritical/ fine grained HAZ. As the type IV damage initiate internally, its initiation cannot be detected using surface techniques such as in-situ metallography. Hence, ultrasonic imaging has been used in the present study for early detection of Type-IV cracking in creep tested modified 9Cr-1Mo ferritic steel weldments.

In order to simulate type IV damage in the steel weldment, various rectangular cross sectional specimens with weld in the centre of the gauge region were subjected to creep tests at 923 K and 50 MPa for different time duration from 527 Hrs to 2820 Hrs (sample ruptured). Ultrasonic C-scan imaging using a 25 MHz immersion focused transducer has been carried out across the weld line in the creep tested specimens in two perpendicular sections of the weldments. Figure 3 shows a b-scan ultrasonic image generated for the first back wall echo obtained on a weld specimen creep tested for 1992 h. Ultrasonic velocity was found to be the minimum (maximum time of flight) in the weld region and increased in the HAZs to reach a maximum (minimum time of flight) in the parent metal. Hence, the HAZs could be differentiated from the weld and parent metals based on the velocity or in-turn the time of arrival of the backwall echo. In the samples creep tested for durations up to 1011 h (~16 % failure strain), no localized damage could be detected. However, in the samples creep tested for more than 1992 h (~50 % failure strain), very high attenuation was observed in one or both sides of the welds in the HAZs (Fig. 3). The location of high attenuation was identified to be towards the parent metal i.e. in the intercritical / fine grained HAZ typical of the type IV cracking. The study clearly demonstrated that ultrasonic measurements can be used for detection of the initiation of the type IV damage, when the damage is still confined internally and no change is observed on the surface.

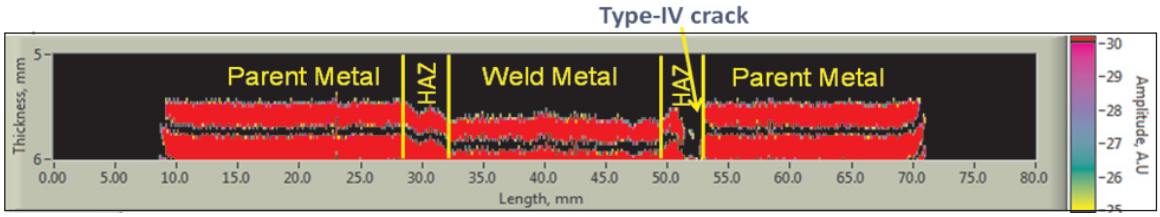

Fig. 3: Ultrasonic b-scan image of the back wall echo across a ferritic steel weld subjected to creep at 923 K / 50 MPa for 1992 h.

Microstructural Characterization in Stainless Steel Using Ultrasonics

Grain Size Measurements in AISI type 316 Stainless Steel

Various ultrasonic methods such as ultrasonic relative attenuation measurement [4], ultrasonic velocity measurement [5] and ultrasonic spectral analysis [3] have been used for the measurement of grain size in AISI type 316 austenitic stainless steel.

For the grain size measurement using ultrasonics, master graph relating ultrasonic velocity with metallographically obtained grain size has been generated (Fig. 4). Using this graph, grain size of new specimens have been obtained. Figure 5 shows the correlation between the grain size values of these new specimens determined using velocity master graph and metallography. The results indicate that grain size can be predicted with a confidence level of 95% using ultrasonic velocity measurements. The grain size estimated by ultrasonic velocity measurements is found to be more accurate as compared to that obtained by conventional attenuation measurements.

Both spectral peak frequency and full width at half maximum (FWHM) of the autopower spectrum of the first back wall echo have been found to decrease with increase in grain size. The spectral peak frequency and FWHM of autopower spectrum are found to be inversely proportional to the square root of the grain size (Fig. 6) and hence these ultrasonic parameters could be linearly correlated with the yield stress of the material. This method of grain size measurement is advantageous because this is applicable to even highly attenuating and thicker materials as only first back wall echo is required to be used. Further, because of its independence on the couplant condition. this methodology has potential for automatic on line measurement of grain size and yield stress, on shop-floor

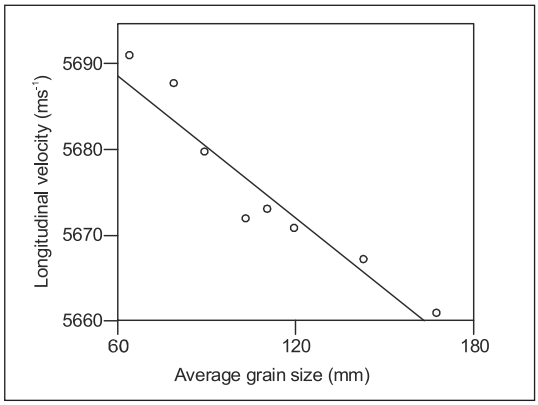

Fig. 4: Variation in ultrasonic velocity with grain size in AISI type 316 stainless steel

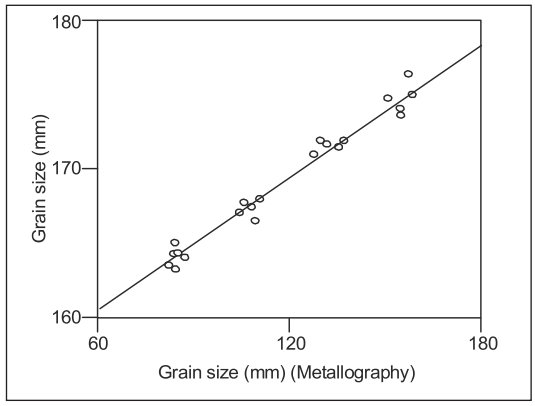

Fig. 5: Comparison of average grain size determined by ultrasonic shear wave velocity with metallographic grain size

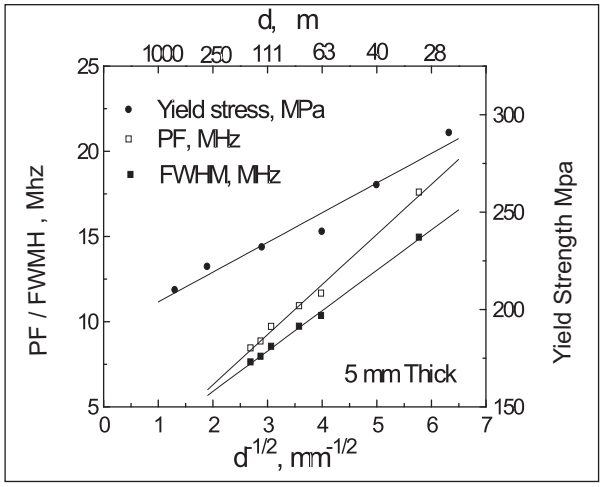

Fig. 6: Variation in yield strength, peak frequency (PF) and FWHM with d-1/2 in AISI type 316 stainless steel.

Imaging of deformation zones in thermomechanically processed alloy D9

Ultrasonic attenuation measurements have been used for imaging the variations in the grain size in 15Cr-15Ni-2.2Mo-Ti modified (D9) austenitic stainless steel specimens thermo-mechanically processed at 1273 K for different strain amplitudes in the range of 0.1 to 0.5 [6]. The study revealed that dynamic recrystallization in 15Cr-15Ni-2.2Mo-Ti modified austenitic stainless steel (alloy D9) initiates after 0.4 strain at 1273 K and appreciable amount of recrystallization is observed only after 0.5 strain at this temperature. Ultrasonic measurements carried out on the specimens thermo-mechanically processed at 1273 K for different strain amplitudes in the range of 0.1 to 0.5 strain could clearly identify recrystallization in the specimens forged to 0.5 strain. Various deformation zones such as intense shear deformation zone (marked as A in Fig. 7), moderate deformation zone (marked as B in Fig. 7) and dead metal zone, could also be imaged using the amplitudes of the first back wall echoes in this specimen (Fig. 7). This could be achieved due to the microstructural variations in those zones. Further, the observation of a single intense shear zone was attributed to the skew (marked as C in Fig. 7) in deformation. The variations in the grain size as revealed by ultrasonic c-scan imaging are substantiated by the optical and scanning electron microscopy studies, thus bringing out the capabilities of nondestructive ultrasonic measurements for evaluation of forged materials.

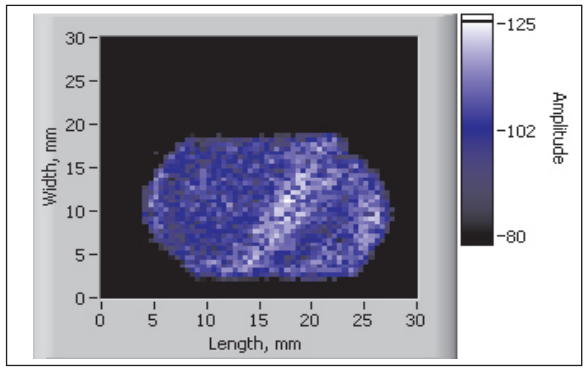

Fig. 7: C-scan image of the specimens forged at 1273 K to a stain of 0.5.

Precipitation Studies in Nuclear Grade AISI type 316LN Stainless Steel

Nitrogen alloyed austenitic stainless steels are potential materials for a variety of engineering applications by virtue of their superior mechanical and chemical properties as compared to other austenitic stainless steels such as 304L, 304, 316 etc. The vastly improved properties of nitrogen steels result from the higher binding energies of nitrogen with chromium and greater pinning effects of dislocations, compared to carbon steels. Addition of nitrogen leads to stronger influence of the thermo mechanical history and the microstructures on the material properties, since the thermo-mechanical history controls the nitrogen distribution in the steel. The various stages of nitrogen repartitioning and precipitation in nuclear grade 316LN stainless steel on aging at 1123 K have been characterised using Transmission Electron Microscopy (TEM). The formation of Cr N clusters on aging for 10h, followed by intra granular precipitation of coherent Cr2N beyond 25 h and finally

the cellular precipitation of Cr2N and formation of chi phase beyond 500h have been well studied and reported. An attempt has been made to correlate these microstructural changes with ultrasonic velocity measurements [5].

Ultrasonic velocity measurements were performed on nuclear grade 316LN stainless steel under various heat treatment conditions. Figure 8 shows the variation in velocity with ageing treatment for longitudinal wave frequencies 10, 25, 50 and 75 MHZ. It is seen that ultrasonic velocity increases up to 25 h of ageing and further ageing at the same temperature till 2000 h decreases the velocity. No difference in the trends is observed between the velocities of all the four frequencies studied. The increase in velocity during 10 h of ageing (stage-A) is mainly associated with matrix effects. Formation of Cr-N rich clusters after 10 h of ageing leaves behind a relatively nitrogen depleted and consequently strain free matrix. Formation of coherent intra granular Cr2N precipitates on ageing up to 25 h is also associated with a small increase in velocity (stage-B). This can be attributed mainly due to modules effects, arising from the large elastic moduli difference between the matrix and the precipitate.

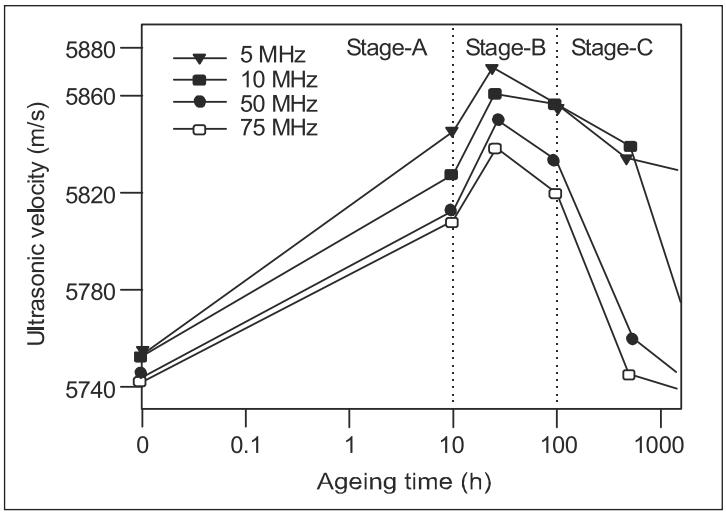

Fig. 8 Variation of velocity with ageing

Formation of cellular precipitates beyond 500 h and coarse phases beyond 1000 h result in increased scattering at the precipitate/matrix interface boundaries and thereby decrease the ultrasonic velocity (stage-C). A larger decrease in velocity with increasing frequency of ultrasonic waves in stage-C, can be seen from Fig. 8. This is because, as the ultrasonic frequency is increased from 5 to 50 MHz, the wavelength decreases by about 10 times. The half wavelength of 50 MHz ultrasonic waves being about 58 m is almost equivalent to the austenite grain size. Since the cellular precipitate extends over the entire grain, a 50 MHz wave would have greater probability of interacting with these precipitates and consequently would undergo greater scattering than a 5 or 10 MHz wave. Consequently, the significant difference between the velocities of the waves with different frequencies, particularly beyond 500 h of ageing as seen from Fig. 8 can be understood well. The

analysis suggests that ultrasonic evaluation may be a handy tool to study the precipitation reaction involving interstitial elements like nitrogen, because precipitation mechanisms are associated with large changes in the lattice strains.

Assessment of Texture in AISI type 304 Stainless Steel

Ultrasonic velocity measurements have been found to be useful for assessment of the degree of cold work and for determination of texture coefficients [7]. The three longitudinal velocities V11, V22 and V33 (Fig. 9a) and the six shear velocities V12, V21, V23, V32, V 31 and V13 (Fig. 9b) have been measured and used to compute the fourth order expansion coefficients (FOEC) of the orientation distribution function (ODF). The longitudinal velocity in the rolling direction (V11) decreased continuously with increase in the cold work, the reduction being 2.4% after 50% cold work. Initially the longitudinal velocity in transverse direction V22 increased for 10% cold worked specimen as compared to solution annealed specimen followed by a reduction in V22 till 27% cold work and thereafter an increase in V22. The velocity in the normal direction V33 decreased up to 20% cold work and further cold working resulted in an increase in the V33. All the six shear velocities decreased with increase in cold work. The shear wave velocities V23 and V32 showed highest decrease followed by V12 and V21 and then followed by V13 and V31. Considering the ease with which the velocities of longitudinal and shear wave propagating in the normal directions can be measured, the ratios V33/V31, V33/V32 and V31/V32 are estimated. A large increase in the velocity ratio V33/V32 was found, increasing almost linearly with increase in the cold work. These ratio parameters do not require measurements of thickness of the specimen.

Figure 9c shows the variation in the three computed FOEC of the ODF. The expansion coefficients C411 and C412 decrease almost linearly with increase in cold work. The nonlinear behaviour for C413 is attributed to the formation of ?1- martensite. Therefore, while using ultrasonic velocities of different wave modes for determination of texture coefficients, the influence of strain-induced phase transformation on ultrasonic velocity should also be taken into account.

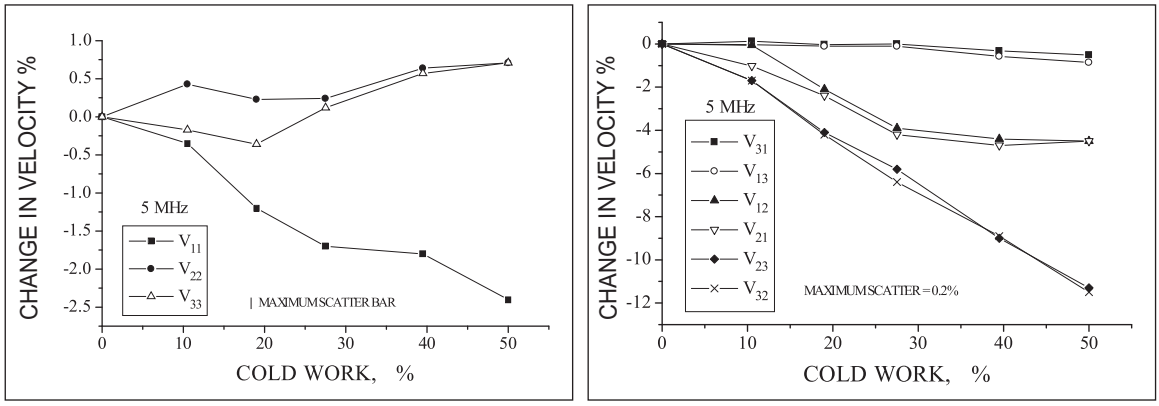

(a) **(b)**

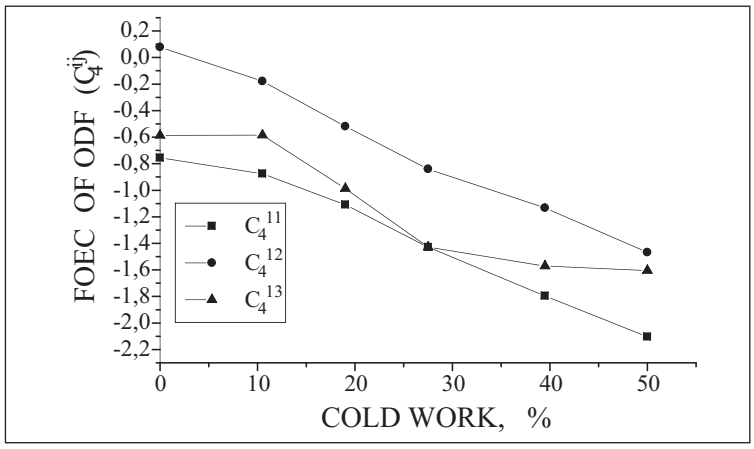

(c)

Fig. 9: Variations in (a) ultrasonic longitudinal velocities (b) shear velocities and (c) FOEC of the ODF with cold work.

Annealing Behavior of Cold Worked Alloy D9

The properties and special characteristics of a given material should be considered while choosing a particular technique for studying annealing behaviour. Recovery, recrystallization and grain growth are the three stages of annealing process which bring out the changes in the cold worked microstructure. Among these stages, recrystallization is the microstructural process by which new strain free grains form from the deformed microstructure. Depending on the material, recrystallization is often accompanied by other microstructural changes like decomposition of solid solution, precipitation of second phases, phase transformations, etc. These changes influence the course of the recrystallisation and often mask the influence of recrystallisation from the information revealed by certain methods of analysis. The most common techniques used to study annealing behaviour of metals and alloys are the hardness testing and optical metallography. These techniques are often found to give different values for the temperature or the time at which the recrystallization process either starts or is completed.

Ultrasonic velocity measurements using 4MHz shear waves were carried out on 20% cold worked (tensile pulled) and annealed specimens of 15Cr-15Ni-2.2Mo-Ti modified austenitic stainless steel (alloy D9) to characterize the isothermal annealing behavior [8]. Shear velocity measurements have been made in all possible directions with reference to cold worked and wave polarisation directions. Three velocity ratio parameters (VS3-VS2)/VS3, (VS3-VS1)/VS3 and (VS2-VS1)/VS2 were established and plotted against the annealing temperature. In the velocity ratio parameters, VS1 is the shear wave velocity measured parallel to the tensile pulling direction, VS2 is the shear wave velocity measured perpendicular to tensile pulling direction but polarization parallel to the pulling direction and VS3 is the velocity perpendicular to the tensile pulling direction with wave polarization perpendicular to the tensile pulling direction. A velocity parameter (VS3-VS1)/VS3, which is a combination of the shear wave velocities measured in the transverse direction with

polarization directions parallel and perpendicular to the cold worked direction was found to closely represent the extent of recrystallization (Fig. 10a). Use of velocity parameters avoid the necessity for specimen thickness measurements which are prone to error or may not be possible. Figure 10b shows the variation in velocity ratio parameter with fraction of recrystallized microstructures. It has been found from these studies that the velocity measurements could sense the onset, progress and completion of recrystallization more accurately compared with that of hardness and strength measurements. It has also been found that the variation in velocity with annealing time is similar at different frequencies (2,10,20 MHz) of the ultrasonic waves used for velocity measurements.

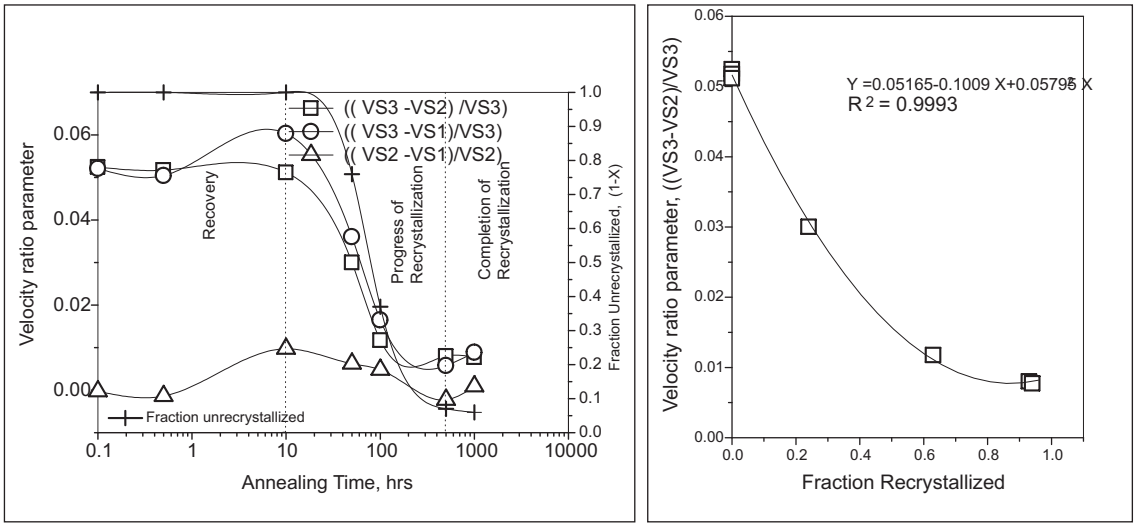

Fig. 10: Variations in (a) velocity ratio parameter and the fraction unrecrystallised microstructure as a function of annealing time at 1073 K and (b) velocity ratio parameter with fraction of recrystallization in alloy D9.

Residual Stress Measurements in Welds of PFBR Main Vessel Sector

The knowledge of residual stresses in engineering structures is important for ensuring their reliable performance, structural integrity and life assessment and extension. Welded components are of major concern as it is well known that welding processes generate considerable residual stresses that are detrimental to the performance of the components. Several destructive, semi destructive and non destructive techniques are in use for the quantitative assessment of residual stresses in welded joints. Ultrasonic non-destructive techniques are useful for the assessment of surface, sub-surface and bulk residual stresses. Critically reflected longitudinal wave (LCR) transit time measurements have been carried out on AISI type 304 stainless steel weld joint in the PFBR main vessel mock-up sector in the longitudinal direction using carefully designed transducer-wedges, which generate and receive LCR waves. Austenitic stainless steel weld joint of the main vessel considered in this study is Single "V" and 35 mm thick weld joint. The transmitter-receiver assembly

was moved over the weld centre and parent metal regions and measurements were taken in the direction parallel to the weld joint. Transit time measurements were made in steps of 2 mm as a function of distance from the weld centre. By using the predetermined value of the acoustoelastic constant (AEC) for AISI type 304 stainless steel, the residual stresses are obtained using the formula V = Vo + A?, where V is the velocity in the presence of stress ?, Vo is the stress free velocity and A is the AEC. Since the measurements were done with a fixed distance between the transmitter and receiver, the velocity term can be replaced by the equivalent transit time in the above equation. Correspondingly, the AEC for the material and probe assembly combination has been obtained as 0.35 nsec/ MPa. Figure 11 shows the variation in residual stress across the weld region. It is seen from Fig. 11 that maximum tensile residual stress occurs at the weld centre and the maximum compressive stress occurs around 25 mm away (heat affected zones) on either side of the weld regions. Quantitative estimation of residual stresses also aids in optimization of the FEM based analysis for prediction of residual stresses and performance evaluation of welded components.

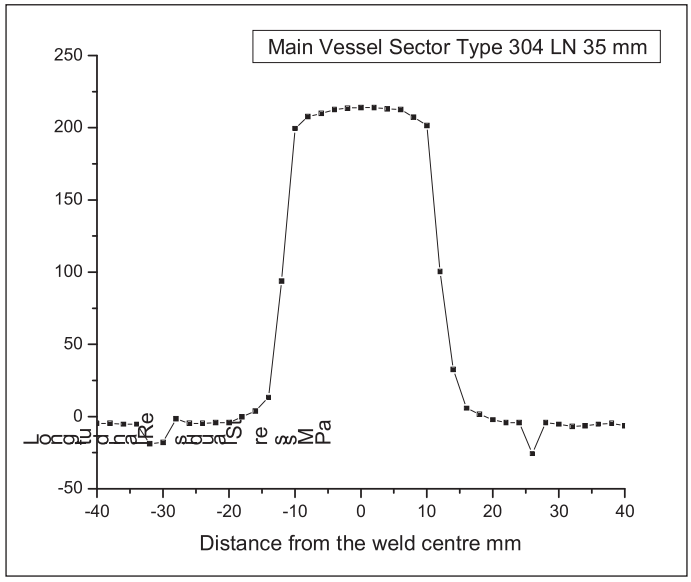

Fig. 11. Variation in longitudinal residual stress in 35 mm thick single "V" AISI type 304 stainless steel weld region as determined by the LCR wave transit time measurements.

Magnetic & Electromagnetic Techniques for Characterization in tainless Steel

Magnetic techniques for assessment of deformation induced martensitic transformation in stainless steel

When magnetic hysteresis loop measurement is made on a material having ferro-magnetic second phase dispersed in a paramagnetic matrix or vice versa, the hysteresis loop shape would reflect the changes in the ratio of the ferromagnetic to nonferro-magnetic phases. Magnetic hysteresis

loop measuerments were carried out on AISI type 304 stainless steel specimens with 0 50 % cold work [7]. It was found that the hysteresis loop shears with increase in cold work and was attributed to the demagnetisation effect due to the presence of magnetic dipoles on the surface of the ferromagnetic second phase (-martensite). The observed increase in coercivity with the increase in the degree of cold work was attributed to the generation of stronger barriers through the deformation of already formed martensite and the increased amount of dislocation density. The slope of the hysteresis loop given by V/ H was measured for different cold worked specimens. The variation of this slope showed that the slope increases with increase in the degree of cold work. Since the H is same for all the specimens, the increase in the V/ H indicates that the intensity of magnetisation (I) increases with increase in the degree of cold work. This is attributed to the increase in the amount of martensite with increase in the degree of cold work. The digitised induced voltage (V) from the coil was rectified and then integrated over the full cycle of the magnetisation using a microcomputer and the variation in this parameter (Vdt) with percent cold work showed that the integrated area of the induced voltage signal increases with increase in the degree of cold work. The variations in both V/ H and the area of the hysteresis loop with degree of cold work are very similar indicating that both these parameters can be used to determine the amount of martensite formed with the increase in the degree of cold work. These two parameters can detect ' martensite even in specimens cold worked for as small as 10%.

Identification of Weld Centre Line using Eddy Current Technique

Austenitic stainless steel welds generally contain a small amount of delta ferrite to prevent hot-cracking. The electrical conductivity and permeability of the weld differ from the base metal due to the presence of the ferromagnetic delta ferrite and hence this variation can be used for identification of the weld centre line using eddy current technique. Identification of weld centre line is necessary for fixing the required skip distance and scan ranges for ultrasonic testing of the welds. For this application, high temperature ECT probe has been developed, which has been tested to work upto 2000C. Figures 12a and b show the scanning of the hot weld plate using high temperature ECT probe and the eddy current based image of the weldment respectively. Due to predominant variations in the electrical conductivity and magnetic permeability (due to the presence of delta ferrite), the weld region has been distinctly noticed in the eddy current images. The weld centerline could be determined with an accuracy of 0.5 mm.

Detection and Evaluation of Sensitisation and Intergranular Corrosion in Austenitic Stainless Steel by Eddy Current Testing (ECT) Technique

Stainless steels have excellent corrosion resistance when properly heated and used in a low temperature environment. However, they are vulnerable to corrosion when exposed to temperatures between 450 and 900 °C. This is because the formation of Cr-rich carbides at the grain boundaries extracts chromium from the grain boundaries and neighboring matrix, leaving a Cr-depleted zone extending to both sides of the grain boundaries. The Cr-depleted zone is vulnerable to attack,

leading to intergranular corrosion (IGC) or stress cracking corrosion (IGSCC). In these steels, IGC and IGSCC are evaluated as per ASTM A262-E followed by a 180 degree bent test or EPR (ASTM G108) tests. For early detection and characterisation of intergranular corrosion, in other words, degree of sensitisation (DOS), an eddy current NDT method has been developed. Eddy current (EC) signal amplitude was found to be a good parameter to monitor the DOS and hence, the propensity for IGC attacks. Investigations were carried out to establish applicability of ECT to quantify DOS in AISI type 316 SS, subjected to aging treatments at 873, 973 and 1073 K for durations ranging from 15 minutes to 25 hours and then exposed to Strauss test as per ASTM A262 Practice E [9]. EC signal amplitudes were determined for as-aged and Strauss test exposed specimens. After the bend test, all the specimens were visually examined. According to the severity of the crack developed, the specimens were classified into four categories, viz. (1) unaffected, (2) formation of micro-fissures, (3) macro-cracks and (4) broken. These four categories of specimens were then compared with the EC responses, in the as-aged condition and Strauss-tested condition (prior to bending) and the EC responses are shown in Figs. 13 a and b respectively. From the comparison of EC signal amplitude with different category specimens, the propensity of IGC can be assessed without subjecting the specimens to bend test. In service, when the components undergo IGC/IGSCC, they are expected to go through the stage of selective attack at grain boundary region before failure occurs. Hence, monitoring of the regions susceptible to IGC/IGSCC by EC testing would provide vital information on the initiation and progress of IGC/IGSCC.

Fig. 12 (a) Scanning of the hot weld plate using high temperature ECT probe

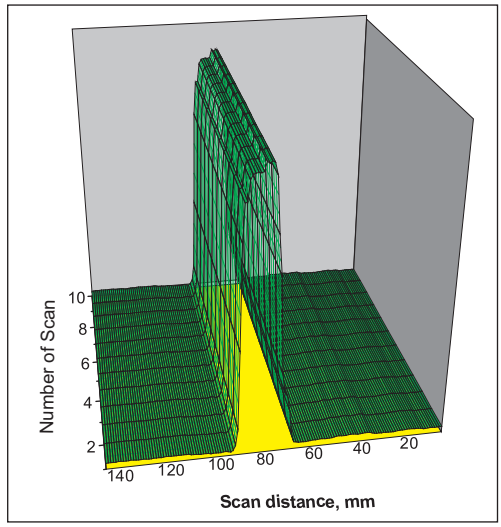

Fig. 12 (b) High temperature ECT based image of the weldment.

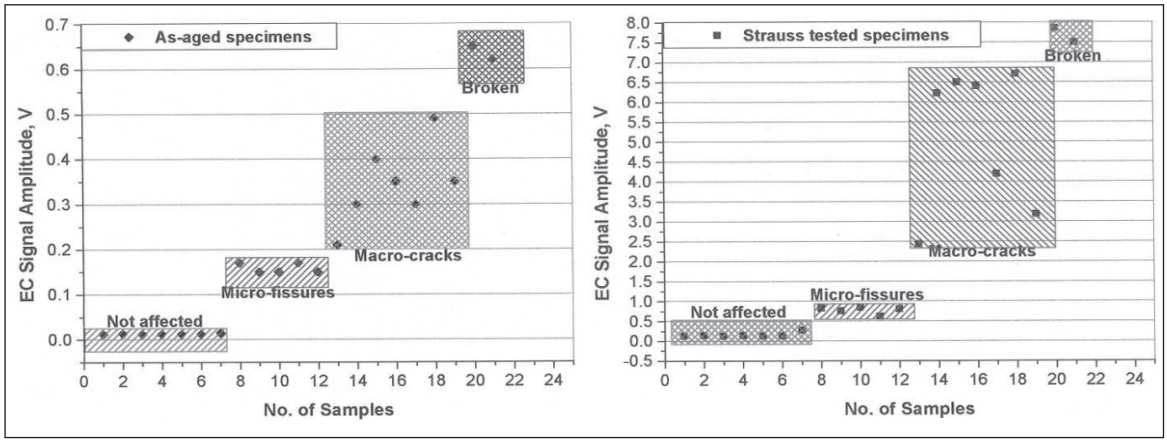

(a) (b)

Fig. 13. Eddy current signal amplitude obtained from the specimens in (a) as-aged and (b) Strauss tested conditions.

Conprehensive Characterization of Ageing Behaviour in M250 Maraging Steel using Multi-NDE Technique

M250 grade maraging steel, by virtue of its excellent mechanical properties i.e. ultra-high yield strength combined with good fracture toughness, is the preferred structural material for critical applications in advanced technologies. In addition to the above mentioned properties, its high strength to weight ratio, good weldability and easy machinability in the solution annealed condition and dimensional stability during aging make this material as an ideal choice for critical rocket motor casing applications in aerospace industries. The strength in aged condition is derived from the fine and coherent intermetallic precipitates, whereas low carbon martensitic structure provides the high fracture toughness. Over-aging results in coarsening of the intermetallic precipitates in addition to the reversion of martensite to austenite. These two processes that occur due to overaging affects both tensile and fracture properties of these steels. Hence, characterization of microstructure plays an important role in qualification of fabricated components for service. Particularly, non destructive evaluation (NDE) techniques are most sought as they provide fast and reliable means of characterizing microstructures of actual components.

Various NDE techniques, such as ultrasonic [10], magnetic Barkhausen emission (MBE) [11], positron annihilation spectroscopy [12] and X-ray diffraction [13] have been used for comprehensive characterization of microstructural features generated by ageing the solution annealed maraging steel M250 at 755 K for duration in range of 0.25-100 h. Each technique provided complimentary information with regard to complex microstructural features that existed in the aged maraging steel specimens. Ultrasonic parameter was found to be more sensitive to the

precipitation of intermetallics, whereas MBE could clearly identify the onset of austenitic reversion. Positron annihilation spectroscopy (PAS) could clearly identify the reduction in defect structure due to reduction in dislocation density during initial durations of ageing of the steel, in addition to the precipitation in complex microstructure during longer aging hours. XRD studies were used for determination of amount of reverted austenite. The present study has clearly brought out the complementary nature of these techniques for comprehensive characterization of ageing behaviour in maraging steels

Characterization of precipitation of intermetallics using ultrasonic velocity measurements [10]

Figure 14 shows the variations in hardness, ultrasonic longitudinal wave velocity and positron annihilation parameter (S parameter) with aging duration. The initial increase in hardness up to 3 h is attributed to the precipitation of Ni3Ti intermetallic precipitates from the martensite matrix as evident from TEM studies. The detailed TEM results are reported elsewhere [10]. The continuous increase in the hardness at intermediate durations (10-40 h) is attributed to additional precipitation of fine Fe2Mo precipitates from the solid solution. The decrease in the hardness upon ageing for longer durations is attributed to the formation of soft reverted austenite phase.

The ultrasonic velocity exhibited similar variation to that of hardness with aging time. Ultrasonic velocity increased linearly with hardness up to 616 VHN corresponding to 10 h of aging. Beyond 10 h of ageing, the ultrasonic velocity changes substantially with a small change in hardness. After reaching the maximum hardness of 673 VHN corresponding to 40 h of aging, ultrasonic longitudinal wave velocity drops significantly with substantial drop in hardness. The initial increase in ultrasonic velocity is attributed to the precipitation of mainly Ni3Ti intermetallic phase, which increases the hardness up to 616 VHN. The increase in the velocity is attributed to the increase in modulus of the matrix due to depletion of solute elements (Ni and Ti) from matrix during precipitation of Ni3Ti. This can be inferred by comparing the Young's modulus of pure iron and M250 steel. Young's modulus of pure iron is about 214 GPa and the addition of alloying elements to Fe to form M250 maraging steel decreases the modulus to 175 GPa. The variation in ultrasonic longitudinal wave velocity and hardness with ageing time could reveal various stages of precipitation and reversion of austenite; however the initiation of the reversion of austenite at 30 h of ageing could not be identified by ultrasonic velocity measurements. Though TEM studies revealed the initiation of reversion of austenite at 30 h itself, decrease in hardness and ultrasonic longitudinal wave velocity is observed only after 40 h. This is attributed to the fact that the precipitation of Fe2Mo, which tends to increase the hardness and velocities, continues to take place in parallel with the phenomenon of reversion to austenite. Hence, decrease in the hardness and ultrasonic longitudinal wave velocity due to formation of austenite can be felt only when this decrease is more than the increase in these parameters due to continued Fe2Mo precipitation. Drastic drop in velocity for longer aging duration is attributed to the formation of reverted austenite.

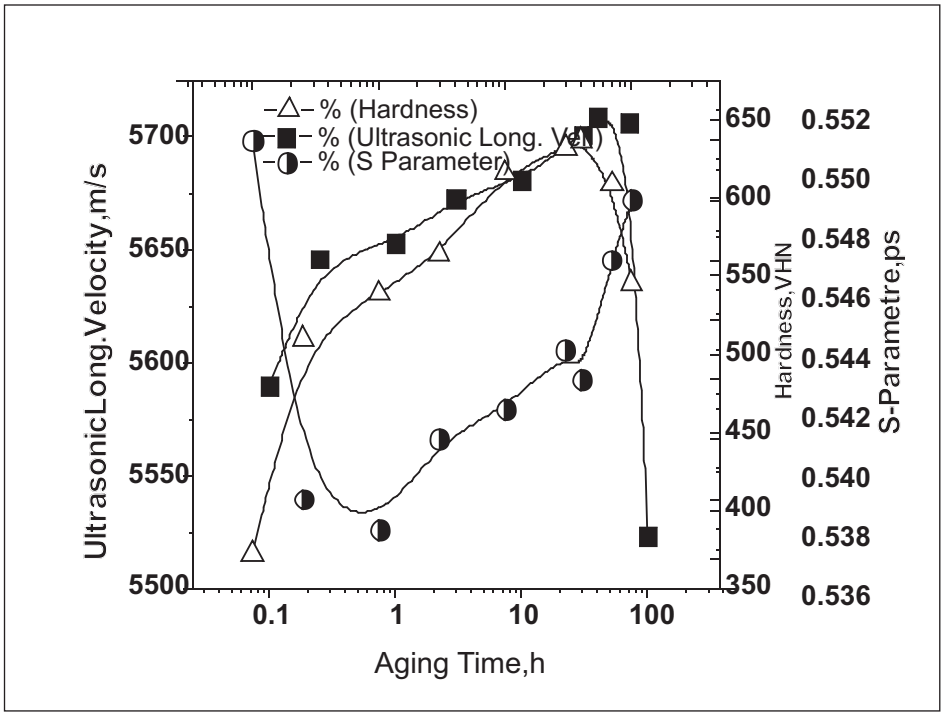

Fig. 14: Variation in hardness, ultrasonic wave velocity and Positron Annihilation (S Parameter) with aging at 755 K.

Characterization of defect structure using Positron Annihilation [12]

Unlike hardness and ultrasonic velocity, S parameter drastically decreases upon ageing for durations upto 1 h, and increases continuously beyond this upto 100 h of ageing (Figure 14). The initial decrease in S parameter upto 1 h of ageing clearly indicates that the defect density of lattice decreases. The decrease in S-parameter in the initial regime (upto 1h) of aging is attributed to two simultaneous mechanisms i.e the reduction in dislocation density due to martensitic recovery and predominantly the precipitation of intermetallics preferentially on dislocations, which results in decrease in trapping sites for positrons, thereby decreasing the S parameter. On the other hand, coarsening of precipitates leads to interface acting as acts trapping sites due to the associated strain field, which results in the increase in S parameter. Since the two processes affect the S parameter in opposite way, the net effect is manifested, as its continuous decrease up to 1 h showing that the reduction in defect structure as the dominant feature beyond which the coarsing of the precipitates is found to be dominant factor. Though at longer ageing durations (30-100 h), reversal of austenitic also take place, the S parameter seems to be subtly of affected by the same as this is only a structural change. The continuous increase in S parameter up to 100 h is the result of continuous precipitation, which acts as trapping sites for positrons.

Detection of reversion of austenite using magnetic Barkhausen emission [11]

Figure 15 show the variations in hardness, MBE RMS, Vol% of austenite and ECT RMS value with aging duration. The variations in the ECT RMS with aging time exhibit similar trends as that of the volume of austenite determined from XRD. They were initially constant and increased drastically at longer aging time. In contrary, the MBE RMS value remained constant initially and drastically dropped at longer aging duration.

Figure 15 also shows the variation in MBE peak heights and volume % of reverted austenite with ageing duration for the isothermally aged specimens at 753 K. The MBE peak height remains almost constant up to 10 hr of aging. Beyond this, substantial drop in MBE rms was observed on aging up to 100 h. In solution annealed condition it is characterized by high dislocation density hence pose serious barriers for domain walls.

MBE rms remains almost constant up to 10 h regime showing that the increase in MBE RMS due to dislocation annihilation is compensated by decrease in MBE RMS due to precipitation of intermetallic phases. Hence a net manifestation of constant voltage is obtained. Beyond 10 h of ageing, the substantial decrease in MBE rms is attributed to the formation of reverted austenite due to dissolution of Ni rich precipitates. Interesting observation is that the onset of austenitic reversion is picked up sensitively by MBE whereas it requires appreciable amount to be detected by XRD (~2% at 40 h). Other wise determinations of this austenite reversion require support of TEM. The increase in austenite from 30 h to 100h is evident from XRD. From Fig. 15, it is also evident that upon 40 h, 70 h and 100 h of ageing, the volume of austenite increases continuously as 2, 6 and 30 % respectively. The substantial decrease in MBE with reversal of austenite is attributed to the fact that the nonmagnetic austenite poses serious domain wall restriction in addition to reducing the total domains taking part in magnetization. Hence we could conclude the MBE technique is very sensitive to characterize austenitic reversion.

The comprehensive results of the present study are summarized below in table 1 for better understanding and discussion. In order to grade the sensitiveness of techniques for various microstructural features the grades were given accordingly wherein 'Y' stands for sensitive, 'YY' stands for 'Highly sensitive' and N stands for 'Not sensitive'. It can be clearly visualized that no technique can completely characterize the microstructural changes occurring upon ageing the solution annealed maraging steel. Hence complimentary information can be obtained from them for comprehensive characterization of microstructural feature. Ultrasonic velocity showed good promise in characterizing the precipitation process and was able to pick up the austenite information to some extent. Its drawback came with respect to obtaining any information about the defect structure and initiation of austenite reversal. Hence, this technique is found to be very sensitive to monitor the precipitation behaviour. Positron annihilation studies were found to be very sensitive to defect structure and precipitation to some extent. The austenite reversion had subtle effect. Hence this technique can be used for high sensitive characterization of defects such as vacancies or dislocations. Magnetic Barkhausen emission could be very effectively used for the detection of onset of austenite reversal.

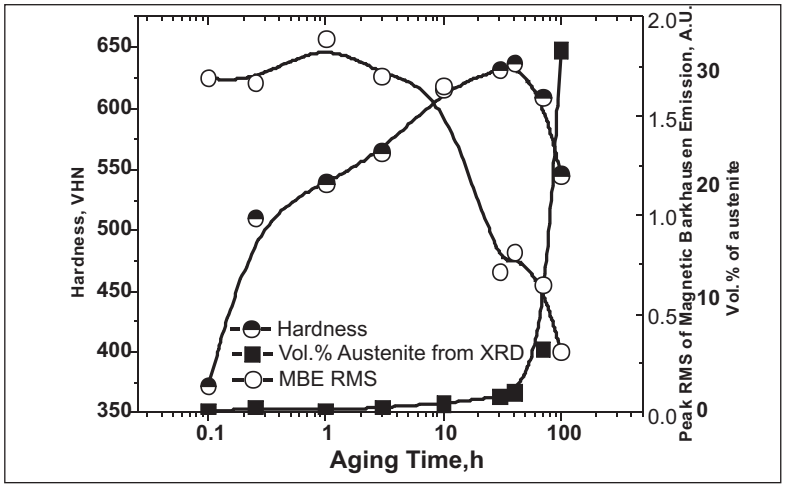

Fig. 15. Variation in hardness, magnetic barkhausen emission Peak RMS and volume % of austenite determined by XRD with aging at 755 K.

Table 1: Summary of the Sensitiveness of Different NDE techniques

NDE Parametres	Defects(Vacancy dislocation)	Precipitates	Reverted Austenite
Ultrasonic Velocity	N	YY	Y
Positron Annihilation	YY	YY	N
Magnetic Barkhausen	Y	Y	YY
XRD	N	N	Y

Concluding Remarks

The nondestructive methodologies developed at the authors' laboratory for characterization of microstructural features in various steels such as ferritic, austenitic stainless and maraging steels have been discussed in the present paper. One or the combinations of various nondestructive evaluation parameters such as ultrasonic velocity, ultrasonic attenuation, spectral analysis of the ultrasonic signals, magnetic Barkhausen emission (MBE), positron annihilations and eddy current amplitude have been judiciously selected for characterization of various microstructural and substructural features such as grain size, precipitation behaviour, texture, recrystallization, thermomechancial processing, degree of sensitization, reversion of martensite to austenite, reversion of austenite to martensite and assessment of residual stresses in different steels. The comparative advantages of various techniques for characterization of specific microstructural features are highlighted. Ultrasonic velocity has been found to be very effective in characterization of precipitation of intermetallic phases in ferritic, austenitic and maraging steels, whereas, electromagnetic techniques are found to be very effective for characterization of reversion of martensite in austenitic steel, reversion of austenite in maraging steel and detection of delta ferrite in austenitic stainless steel weldments. In this paper, the emphasis is given on the judicious selection of a single NDE technique/

parameter or multi-technique/ multi-parameteric approach for comprehensive characterization of microstructural/ substructural changes occurring in steels, based on the in-depth understanding of the materials response to the specific form of energy imparted during NDE.

Acknowledgement

Authors are thankful to many colleagues in the Metallurgy and Materials Group of Indira Gandhi Centre for Atomic Research for their contributions.

Reference

1. Raj B, Moorthy V, Jayakumar T, Rao K. Assessment of microstructures and mechanical behaviour of metallic materials through non-destructive characterisation. International materials reviews. 2003;48(5):273-325.
2. Kumar A, Laha K, Jayakumar T, Rao K, Raj B. Comprehensive microstructural characterization in modified 9Cr-1Mo ferritic steel by ultrasonic measurements. Metallurgical and Materials Transactions A. 2002;33(6):1617-1626.
3. Kumar A, Jayakumar T, Raj B. Ultrasonic spectral analysis for microstructural characterization of austenitic and ferritic steels. Philosophical Magazine A. 2000;80(11):2469-2487.
4. Palanichamy P, Joseph A, Jayakumar T. Grain size measurements in austenitic stainless steel using ultrasonics. Insight. 1994;36(11):874-877.
5. Palanichamy P, Joseph A, Jayakumar T, Raj B. Ultrasonic velocity measurements for estimation of grain size in austenitic stainless steel. NDT & E International. 1995;28(3):179-185.
6. Mandal S, Kumar A, Sivaprasad PV, Jayakumar T, Raj B. Characterisation of microstructural evolution during thermomechanical processing of 15Cr-15Ni-2.2Mo-Ti modified austenitic stainless steel (alloy D9) using ultrasonic measurements. Materials science and technology. 2007;23(11):1381-1386.
7. Jayakumar T, Mukhopadhyay CK, Kasiviswanathan KV, Raj B. Acoustic and magnetic methods for characterisation of microstructures and tensile deformation in AISI type 304 stainless steel. Transactions of the Indian Institute of Metals(India). 1998;51(6):485-509.
8. Palanichamy P, Vasudevan M, Jayakumar T, Venugopal S, Raj B. Ultrasonic velocity measurements for characterizing the annealing behaviour of cold worked austenitic stainless steel. NDT & E International. 2000;33(4):253-259.
9. Shaikh H, Sivaibharasi N, Sasi B, Anita T, Amirthalingam R, Rao BPC, Jayakumar T, Khatak HS, Raj B. Use of eddy current testing method in detection and evaluation of sensitisation and intergranular corrosion in austenitic stainless steels. Corrosion science. 2006;48(6):1462-1482.
10. Rajkumar KV, Kumar A, Jayakumar T, Raj B, Ray KK. Characterization of aging behavior in M250 grade maraging steel using ultrasonic measurements. Metallurgical and Materials Transactions A. 2007;38(2):236-243.
11. Rajkumar KV, Vaidyanathan S, Kumar A, Jayakumar T, Raj B, Ray KK. Characterization of aging-induced microstructural changes in M250 maraging steel using magnetic parameters. Journal of Magnetism and Magnetic Materials. 2007;312(2):359-365.
12. Rajkumar KV, Rajaraman R, Kumar A, Amarendra G, Jayakumar T, Sundar CS, Raj B, Ray KK. Investigation of microstructural changes in M250 grade maraging steel using positron annihilation. Philosophical Magazine. 2009;89(20):1597-1610.
13. Mahadevan S, Jayakumar T, Rao BPC, Kumar A, Rajkumar KV, Raj B. X-Ray Diffraction Profile Analysis for Characterizing Isothermal Aging Behavior of M250 Grade Maraging Steel. Metallurgical and Materials Transactions A. 2008;39(8):1978-1984.